

of the radical pair **2d**/ArO• (Scheme II). A search for further support of the nitroxyl radical flavoenzyme mechanism remains for future investigation.

Acknowledgment. We thank Professor William Orme-Johnson for advice and assistance with ESR spectroscopy and Dr. C. Costello and E. Block for mass spectra. We also acknowledge Professors C. Walsh and T. C. Bruice and Dr. R. Spencer for their interest and insightful discussions. This work was funded by the National Institutes of Health (Grant CA20574) and the Alfred P. Sloan Foundation.

Laser Synthesis of Metal Clusters from Metal Carbonyl Microcrystals

M. A. Duncan, T. G. Dietz, and R. E. Smalley*

*Rice Quantum Institute and Department of Chemistry
Rice University, Houston, Texas 77001*

Received May 11, 1981

While investigating the photoionization behavior of iron pentacarbonyl in a supersonic beam, we have recently come across evidence for a novel laser photolytic process whereby microcrystals of $\text{Fe}(\text{CO})_5$ are efficiently converted in a single laser shot into Fe_x clusters ($x = 1-30$). This process is remarkable in that it involves (1) wholesale reorganization of the chemical arrangement within a van der Waals bound molecular crystallite prior to vaporization of this crystal and (2) laser excitation in a restricted region of what appears to be an entirely diffuse absorption spectrum. Although the results reported below refer only to ultracold microcrystals of iron pentacarbonyl traveling collision-free at supersonic velocity in a molecular beam, this laser-induced reorganization to Fe_x should also occur within the first 100 Å of the surface of a bulk phase $\text{Fe}(\text{CO})_5$ crystal. Since sublimable carbonyl species are readily available for most of the transition metals, this laser chemistry may offer quite interesting new possibilities for polynuclear metal cluster synthesis on a macroscopic scale.

One of the oldest preparative techniques for multinuclear metal clusters is simply irradiation by direct sunlight.¹ In fact this remains a favored technique for the synthesis of $\text{Fe}_2(\text{CO})_9$ and very recently has been used to produce new cluster species such as $(\eta^5\text{-C}_5\text{H}_5)\text{Nb}_3(\text{CO})_7$.² In the case of $\text{Fe}(\text{CO})_5$, the primary photochemical event in condensed phases is believed to be ejection of CO to form $\text{Fe}(\text{CO})_4$,^{3,4} which is then free to participate in further reactions such as cluster formation.



Addition of more $\text{Fe}(\text{CO})_4$ radicals to produce larger clusters is known to occur, but only when the reaction mixture is heated and then only in small yield. Under normal photolytic conditions the dimer concentration is limited by the fact that metal-metal bond scission is likely the favored primary process.⁵ Prolonged exposure to light will ultimately lead to the decomposition of $\text{Fe}(\text{CO})_5$ to produce bulk metallic iron and CO gas; so it is clear that some mechanisms do exist for the photolytic production of larger clusters. Under conventional conditions, however, these mechanisms are slow and never result in a substantial yield of metal

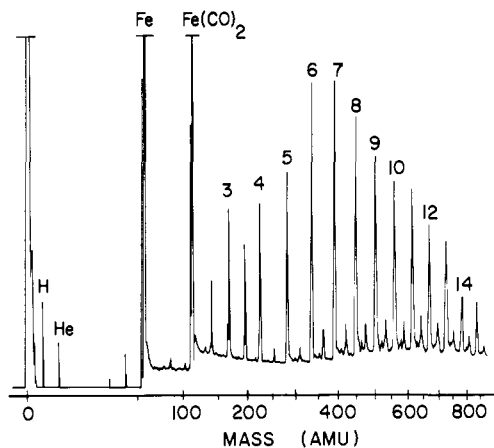


Figure 1. Time-of-flight mass spectrum of ions produced by ArF laser excitation of a $\text{Fe}(\text{CO})_5$ microcrystal beam. Numbered peaks are predominantly due to bare iron clusters. Partially fragmented clusters of the type $\text{Fe}_x(\text{CO})_y$, where y is odd are seen as small peaks between the larger numbered features. Although these large peaks must contain some contribution from the even y clusters, there is no reason to expect a dominance of these even species in the partially fragmented distribution.

clusters of intermediate size. The following experiment indicates that a much more favorable situation exists under intense pulsed ArF excimer laser irradiation.

A metal carbonyl microcrystal beam was produced by pulsed supersonic expansion of 0.2% $\text{Fe}(\text{CO})_5$ in 15 atm of helium from a 0.1-cm diameter orifice at 300 K. The supersonic nozzle used in this work has been described previously.⁶ After careful collimation and differential pumping, the resultant beam passed through a time-of-flight photoionization mass spectrometer⁷ where various lasers were used to photolyze and interrogate the content of the molecular beam. Using an excimer laser operating on the F_2 transition at 1570 Å, the presence of iron pentacarbonyl microcrystals was readily monitored since all crystals larger than $[\text{Fe}(\text{CO})_5]_3$ are directly photoionized at this wavelength to produce primarily ions of the type $[\text{Fe}(\text{CO})_5]_n^+$. However, as shown in Figure 1, drastically different results are observed when the excimer laser is operated on the ArF transition at 1930 Å. The strong mass peaks corresponding to Fe and $\text{Fe}(\text{CO})_2$ shown off scale in this figure are due to multiphoton ionization of $\text{Fe}(\text{CO})_5$ monomer in the beam.⁸ The strong mass peaks numbered from 3 to 14 arise from ArF laser photolysis of the $[\text{Fe}(\text{CO})_5]_n$ microcrystals and occur in the appropriate mass channels for the bare clusters Fe_3 through Fe_{14} . The apparent cluster distribution shown in the figure is distorted by the fact that only one mass is perfectly focused onto the detector at any one time. Mass spectra optimized for larger clusters show the distribution to extend with good intensity out to approximately Fe_{30} .

Generation of these Fe_x clusters was found to be strongly dependent on ArF laser fluence. Halving this fluence from 20 to 10 mJ cm^{-2} reduced the Fe_x cluster intensity by a factor of 20. Excitation with the 4th harmonic of a Nd:YAG laser at 2650 Å failed to produce any significant cluster photoion signal other than the very strong Fe and very weak FeCO and $\text{Fe}(\text{CO})_2$ signals expected from $\text{Fe}(\text{CO})_5$ monomer.⁸ This remained true for all laser fluences from 0–100 mJ cm^{-2} (4-ns pulse). Even though the absorption cross section for $\text{Fe}(\text{CO})_5$ at 2650 Å is only about one-half of that at 1930 Å,⁴ the fluence range explored with the 2650-Å laser was more than sufficient to achieve equivalent energy deposition.

At 20 mJ cm^{-2} , a 10-ns ArF laser pulse will excite $\text{Fe}(\text{CO})_5$ molecules at a rate of roughly $2 \times 10^8 \text{ s}^{-1}$. Microcrystals of less

(1) Speyer, E.; Wolf, H. *Ber. Dtsch. Chem. Ges.* **1927**, *60*, 1424–1425.

(2) Herrmann, W. A.; Biersach, H.; Ziegler, M. L.; Weidenhammer, K.; Siegel, R.; Rehder, D. *J. Am. Chem. Soc.* **1981**, *103*, 1692–1699.

(3) For a review of metal carbonyl photochemistry, see: Wrighton, M. *Chem. Rev.* **1974**, *74*, 401–430.

(4) (a) Nathanson, G.; Gitlin, B.; Rosan, A. M.; Yardley, J. T. *J. Chem. Phys.* **1981**, *74*, 361–369. (b) Yardley, J. T.; Gitlin, B.; Nathanson, G.; Rosan, A. M. *Ibid.* **1981**, *74*, 370–378.

(5) Wrighton, M. S.; Ginley, D. S. *J. Am. Chem. Soc.* **1975**, *97*, 2065–2072.

(6) Liverman, M. G.; Beck, S. M.; Monts, D. L.; Smalley, R. E. *J. Chem. Phys.* **1979**, *70*, 192–198.

(7) Dietz, T. G.; Duncan, M. A.; Liverman, M. G.; Smalley, R. E. *J. Chem. Phys.* **1980**, *73*, 4816–4821.

(8) Duncan, M. A.; Dietz, T. G.; Smalley, R. E. *Chem. Phys.* **1979**, *44*, 415–419.

than 1000 $\text{Fe}(\text{CO})_5$ molecules are optically thin at this wavelength; so this excitation rate applies to all molecules regardless of their position in the microcrystal. Such a rate is sufficient to excite over 80% of the crystal during the laser pulse. At either laser wavelength this degree of excitation is far more than needed to totally vaporize the crystal into separate $\text{Fe}(\text{CO})_5$ molecules or completely reorganize it into an iron cluster plus a rapidly expanding cloud of CO gas. Reorganization is favored in the internal regions of the microcrystal where vaporization is slowed by inertial confinement of the outer layers. Metal cluster growth here competes well with vaporization if the local temperature following absorption of a photon rises above some critical value. For these supersonic microcrystals of $\text{Fe}(\text{CO})_5$, such a threshold appears to lie between 2650 and 1930 Å.

Acknowledgment. We express our appreciation to Drs. Donald Cox and Andrew Kaldor of Exxon Research and Engineering for provocative discussions and providing the excimer laser used in this research. Support from the Department of Energy and The Robert A. Welch Foundation is gratefully acknowledged.

New Layered Compounds with Transition-Metal Oxide Layers Separated by Covalently Bound Organic Ligands. Molybdenum and Tungsten Trioxide-Pyridine

Jack W. Johnson,* A. J. Jacobson,* S. M. Rich, and J. F. Brody

Corporate Research Science Laboratories
Exxon Research and Engineering Company
Linden, New Jersey 07036

Received February 23, 1981

Revised Manuscript Received June 22, 1981

Layered solid compounds consisting of alternating organic and inorganic layers have recently been of interest in a variety of areas due to their sorptive, catalytic, and transport properties.¹⁻⁷ Solids of this type most commonly are formed of negatively charged layers of metal oxide or sulfide and layers of organic cations. Some examples are organoammonium compounds of clay minerals² in which the negatively charged inorganic layers are aluminosilicates and the ammonium molybdenum bronzes³ whose inorganic layers have the double octahedra structure of MoO_3 . More recently,⁴ it has been recognized that organoammonium ions are also constituents of the organic layer in at least some of the amine intercalates of the transition-metal dichalcogenides.⁵ Another series of compounds in which the organic layers are bound in a covalent, rather than ionic, manner to the inorganic layers is the zirconium monoalkyl or monoaryl phosphates and phosphinates in which the organic groups are attached to the zirconium phosphate layers by P-O-C or P-C covalent bonds.⁶ We wish to report new layered compounds of MoO_3 and WO_3 with pyridine and 4,4'-bipyridine that consist of inorganic layers separated by organic layers in which the heterocyclic nitrogen is directly coordinated to the metal atom of the oxide layer. Related materials in which a coordinated organic ligand separate planar inorganic layers are the nickel

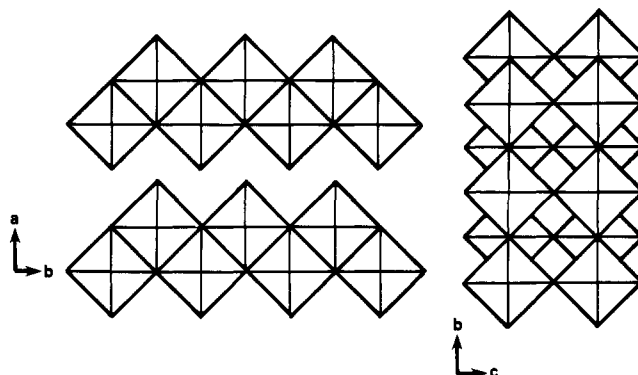


Figure 1. Two views of the structure of MoO_3 . The layers are formed of MoO_6 octahedra that are connected by μ^2 oxygens along c and by μ^3 oxygens along b . The layers are stacked along a and held together by van der Waals contacts of terminal oxygens.

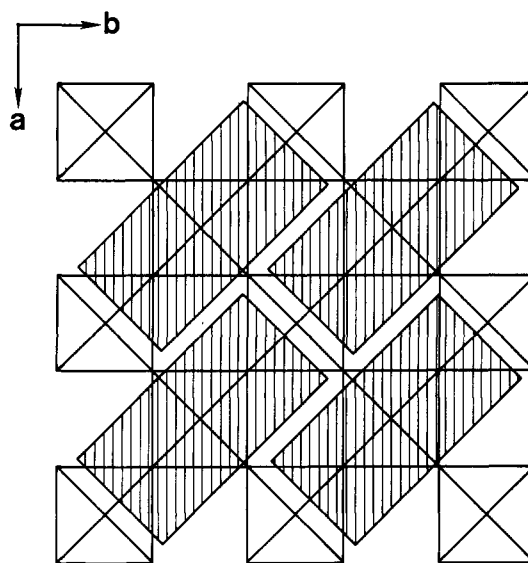


Figure 2. View of the structure of $\text{MoO}_3\text{C}_5\text{H}_5\text{N}$ looking down c upon the layers. The shaded rectangles represent the van der Waals dimensions of the pyridine molecule. To conform to the observed tetragonal symmetry, the pyridine molecules must be disordered by a 90° rotation around the Mo-N bond.

cyanide complexes $\text{NiL}_2\text{Ni}(\text{CN})_4$.⁷

MoO_3 consists of 6.928-Å thick double layers of edge- and corner-sharing octahedra represented by the formula $\text{MoO}_{1/1}\text{O}_{2/2}\text{O}_{3/3}$,⁸ as depicted in Figure 1. When excess pyridine is heated with MoO_3 under strictly anhydrous conditions, microcrystalline $\text{MoO}_3\text{C}_5\text{H}_5\text{N}$ is formed.⁹ Infrared¹¹ and structural data (vide infra) demonstrate that pyridine is directly coordinated

(1) Whittingham, M. S.; Jacobson, A. J. "Intercalation Chemistry"; Academic Press: New York, 1981.

(2) Thomas, J. M.; Adams, J. M.; Graham, S. H.; Tenakoon, D. T. B. *Adv. Chem. Ser.* 1977, No. 163, 298-315.

(3) Schöllhorn, R.; Kuhlman, R.; Besenhard, J. O. *Mater. Res. Bull.* 1976, 11, 83-90. Schöllhorn, R.; Schulte-Nölle, T.; Steinhoff, G. J. *Less-Common Met.* 1980, 71, 71-78.

(4) Schöllhorn, R.; Zagefka, H. D. *Angew. Chem.* 1977, 89, 193-194. *Angew. Chem., Int. Ed. Engl.* 1977, 16, 199-200. Schöllhorn, R.; Butz, T.; Lurf, A. *Mater. Res. Bull.* 1979, 14, 369-376.

(5) Gamble, F. R.; Geballe, T. H. *Treatise Solid State Chem.* 1976, 3, 89.

(6) Alberti, G.; Costantino, U.; Alluli, S.; Tomassini, N. *J. Inorg. Nucl. Chem.* 1978, 40, 1113-1117. Dines, M. B.; DiGiacomo, P. M. *Inorg. Chem.* 1981, 20, 92-97.

(7) Mathey, Y.; Mazières, C.; Setton, R. *Inorg. Nucl. Chem. Lett.* 1977, 13, 1-3. Aragon de la Cruz, F.; Alonso, S. M. *Naturwissenschaften* 1975, 62, 298. Walker, G. F.; Hawthorne, D. G. *Trans. Faraday Soc.* 1967, 63, 166-174.

(8) Hulliger, F. "Structural Chemistry of Layer-Type Phases"; Reidel, D.: Boston, 1976; p 169 ff. The structural formula $\text{MoO}_{1/1}\text{O}_{2/2}\text{O}_{3/3}$ indicates the Mo is octahedrally coordinated by 1 unshared oxygen ($\text{O}_{1/1}$), two O atoms shared with another Mo ($\text{O}_{2/2}$), and three O atoms shared with two other Mo ($\text{O}_{3/3}$). In organometallic notation, the Mo coordination sphere would be represented by $\text{Mo}(\mu^2\text{-O})_2(\mu^3\text{-O})_3$.

(9) Elemental analysis (C, H, N, Mo) and TGA confirmed the stoichiometry. The synthesis is tedious. Prolonged heating (30 days) at 160-180 °C in sealed tubes with intermediate regrinding is necessary to ensure complete reaction of the MoO_3 . The compound has been previously reported¹⁰ but not structurally characterized.

(10) Bernard, J.; Camelot, M. C. R. *Hebd. Seances Acad. Sci., Ser. C* 1966, 263, 1068-1071.

(11) IR (cm^{-1} , intensity): 1644 w, 1603 s, 1573 m, 1540 vw, 1486 m, 1443 vs, 1239 w, 1220 m, 1156 vw, 1141 m, 1062 s, 1041 s, 1012 vw, 1004 vw, 950 w, 931 vs. This spectrum best fits known spectra of pyridine coordinated to a metal atom (Lewis base) site.¹² Particularly, an intense band at ca. 1542 cm^{-1} characteristic of pyridinium ion is almost totally absent.

(12) Matulewicz, E. R. A.; Kerkhof, F. P. J. M.; Moulijn, J. A.; Reitsma, H. J. J. *Colloid Interface Sci.* 1980, 77, 110-119. Perry, E. P. *J. Catal.* 1963, 2, 371-379.